1   **Abrupt climate and vegetation variability of eastern Anatolia during the last glacial**

2   Nadine Pickarski [1,*], Ola Kwiecien [2], Dafna Langgut[3], Thomas Litt [1]

3   [1] *University of Bonn, Steinmann Institute for Geology, Mineralogy, and Paleontology, Bonn, Germany*

4   [2] *Ruhr-University Bochum, Sediment and Isotope Geology, Bochum, Germany*

5   [3] *Tel Aviv University, Institute of Archaeology, Tel Aviv, Israel*

6   [*] Corresponding author. E-mail address: pickarski@uni-bonn.de

7   **Abstract**

8   Detailed analyses of the Lake Van pollen, Ca/K ratio, and stable oxygen isotope record allow the

9   identification of millennial-scale vegetation and environmental changes in eastern Anatolia throughout the

10   last glacial (~111.5-11.7 ka BP). The climate of the last glacial was cold and dry, indicated by low

11   arboreal pollen (AP) levels. The driest and coldest period corresponds to Marine Isotope Stage (MIS) 2

12   (~28-14.5 ka BP), which was dominated by highest values of xerophytic steppe vegetation.

13   Our high-resolution multi-proxy record shows rapid expansions and contractions of tree populations that

14   reflect variability in temperature and moisture availability. These rapid vegetation and environmental

15   changes can be related to the stadial-interstadial pattern of Dansgaard-Oeschger (DO) events as recorded

16   in the Greenland ice cores. Periods of reduced moisture availability were characterized by enhanced

17   occurrence of xerophytic species and high terrigenous input from the Lake Van catchment area.

18   Furthermore, the comparison with the marine realm reveals that the complex atmosphere-ocean interaction

19   can be explained by the strength and position of the westerlies, which are responsible for the supply of

20   humidity in eastern Anatolia. Influenced by the diverse topography of the Lake Van catchment, more

21   pronounced DO interstadials (e.g., DO 19, 17-16, 14, 12 and 8) show the strongest expansion of temperate

22   species within the last glacial. However, Heinrich events (HE), characterized by highest concentrations of

23   ice-rafted debris (IRD) in marine sediments, cannot be separated from other DO stadials based on the

24   vegetation composition in eastern Anatolia. In addition, this work is a first attempt to establish a

25   continuous microscopic charcoal record for the last glacial in the Near East. It documents an immediate

26   response to millennial-scale climate and environmental variability and enables us to shed light on the

27   history of fire activity during the last glacial.

28   **1. Introduction**

29   The last glacial inception was marked by the expansion of continental ice sheets and substantial changes

30   in oceanographic conditions in the North Atlantic as well as in atmospheric temperature and moisture

31   balance in the Northern Hemisphere (e.g., Blunier & Brook, 2001; Cacho et al., 2000, 1999; Chapman and

32   Shackleton, 1999; Rasmussen et al., 2014; Sánchez Goñi et al., 2002; Svensson et al., 2008, 2006; Wolff

33 et al., 2010). Between Marine Isotope Stages (MIS) 5d and 2, the climatic conditions were characterized
34 by numerous abrupt millennial-scale oscillations, known as Dansgaard-Oeschger events (DO; Dansgaard
35 et al., 1993). These are most prominently documented in Greenland ice cores and exhibit an abrupt
36 warming (Greenland interstadials; GI), followed by a gradual cooling and a final rapid temperature drop
37 towards a cold Greenland stadial (GS; e.g., NGRIP members, 2004; Rasmussen et al., 2014; Svensson et
38 al., 2008; Wolff et al., 2010). About 25 such stadial to interstadial transitions, varying in amplitude from
39 5°C to 16°C, are defined in the NGRIP record during the last glacial period (NGRIP members, 2004;
40 Rasmussen et al., 2014; Wolff et al., 2010). Although the climatic and environmental impacts of the DO
41 cycles have been intensively studied during the last decades, the mechanism behind them is still under
42 debate (e.g., Cacho et al., 2000, 1999; Rasmussen et al., 2014; Wolff et al., 2010). The main process
43 proposed as a cause for the recurring pattern is freshwater being forced from ice-sheets that affected the
44 extent of the sea ice, ocean heat transport, and Atlantic Meridional Overturning Circulation (AMOC;
45 Bond and Lotti, 1995; Cacho et al., 2000, 1999; Chapman and Shackleton, 1999; Hemming, 2004; Hodell
46 et al., 2008; McManus et al., 1999; Rasmussen et al., 2014; Wolff et al., 2010). The most extreme cold
47 intervals are Heinrich events (HE; Bond et al., 1993, 1992, Heinrich, 1988), characterized by reduced sea
48 surface temperatures (SST; Cacho et al., 1999) with highest concentrations of ice-rafted debris (IRD) in
49 marine sediments due to massive iceberg discharges, which mainly originated from the Laurentide ice
50 sheet (Alvarez-Solas and Ramstein, 2011).

51 Long-term terrestrial pollen records from the central and eastern Mediterranean, for example several crater
52 lakes in Italy (e.g., Lagaccione, Lago di Vico, Lazio Valle di Castiglione, Stracciacappa; Follieri et al.,
53 1998), Lago Grande di Monticchio (Italy; e.g., Allen et al., 1999), Lake Prespa (between Albania,
54 Republic of Macedonia, and Greece; Panagiotopoulos et al., 2014), Lake Ohrid (Albania; Lézine et al.,
55 2010) and Tenaghi Philippon (Greece; e.g., Müller et al., 2011) demonstrate a clear vegetation response to
56 millennial-scale climate variability during the last glacial. These regions are highly sensitive to short-term
57 vegetation changes as recognized by steppe-dominated open landscapes during stadials and increased
58 range of temperate tree taxa during interstadials (e.g., Allen et al., 2000, 1999; Follieri et al., 1998;
59 Langgut et al., 2011; Lézine et al., 2010; Müller et al., 2011; Panagiotopoulos et al., 2014; Shumilovskikh
60 et al., 2014). In contrast to southern Europe, high-resolution and continuous terrestrial sedimentary records
61 displaying abrupt climate oscillations are rare in the entire Near East.

62 Since the first long lacustrine sediment sequences were recovered at Lake Van in summer 2010 (Litt and
63 Anselmetti, 2014, Litt et al., 2012), numerous high-resolution data have been gathered, providing insight
64 into short-term changes in past climatic and environmental conditions in eastern Anatolia (e.g., XRF
65 measurements described by Kwiecien et al., 2014; total organic carbon content (TOC), Stockhecke et al.,
66 2014a). The sensitivity of this region was already well-documented by previous palynological data sets
67 covering the Late Glacial and the Holocene periods (Litt et al., 2009; Wick et al., 2003). First pollen

68 results of the new ~219 m long composite profile encompassing the last 600 ka, have been described
69 based on lower temporal resolution (between ~900 and 3,800 years) by Litt et al. (2014). A detailed high-
70 resolution pollen analysis (between ~100 and 800 years) for the last interglacial (131.2-111.5 ka BP) is
71 documented in Pickarski et al. (2015).
72 Here we present new biotic data (pollen, microscopic charcoal remains) and combine them with already
73 available Lake Van abiotic proxies (stable oxygen isotope and element measurements) of the last glacial
74 period (~111.5-11.7 ka BP). Special focus is given to the centennial- to millennial-scale climate
75 variability, as known from Greenland, and the regional response of vegetation to abrupt
76 paleoenvironmental changes in eastern Anatolia. After the examination of climate and vegetation changes
77 on a local level, we compare our results to selected global reference archives. Furthermore, we provide the
78 first continuous sedimentary microscopic charcoal record from Lake Van to give insights into the coupling
79 and feedback between fire activity and major changes in climate, vegetation, and fuel amount during the
80 last glacial.

81 **2. Regional setting**

82 Lake Van (38.6°N, 42.8°E) is a deep terminal alkaline lake (3,574 km²; max. depth >450 m) situated on
83 the eastern Anatolian high plateau at 1,647 m above sea level (asl, Fig. 1). It is the largest soda lake in the
84 world (Degens and Kurtman, 1978), which is partly fed by numerous small rivers around the basin. In the
85 south, the lake is surrounded by the Bitlis Massif reaching altitudes of more than 3,500 m asl. Two large
86 active stratovolcanoes, Nemrut (2,948 m asl) and Süphan (4,058 m asl), border the lake to the west and
87 north (Fig. 1B).
88 The present-day climate of eastern Anatolia is controlled by seasonal changes in the position and strength
89 of the following atmospheric components: (a) the mid-latitude westerlies, (b) the sub-tropical high-
90 pressure system, and (c) the Siberian high-pressure system (Akçar and Schlüchter, 2005; Türkeş, 1996).
91 The regional climate at Lake Van is continental with warm/dry summers (mean temperature >20°C;
92 Turkish State Meteorological Service) and cold/wet winters, marked by regular frosts. The minimum
93 average temperature of the coldest month is far below 0°C (-7.9°C in Van; see Fig. 1B for the location).
94 Total rainfall varies from 385 mm/a (Van) to 816 mm/a (Tatvan) and peaks in the winter months (October
95 to February), with a second rainfall maximum during spring (March to May). Higher elevations of the
96 west-east oriented mountain ranges along the Bitlis Massif (Fig. 1B) are affected by the strength and
97 position of the 'Cyprus cyclones' from the Mediterranean Sea with precipitation values up to 1,200 mm/a
98 in Bitlis (Turkish State Meteorological Service; Litt et al., 2014).
99 The modern distribution of vegetation at Lake Van is closely related to rough orography and spatial
100 rainfall variability. The southward slopes of the Bitlis Massif are covered by the Kurdo-Zagrosian oak
101 steppe-forest (*Quercetea brantii*), which extends from the Taurus Mountains (east-central Turkey) via the

102 Bitlis complex (SW shore of Lake Van) to the Zagros Mountains (SW Iran; Zohary, 1973). It consists of

103 several oak species, which are accompanied by *Pistacia atlantica, P. khinjuk, Acer monsplessulanum,*

104 *Juniperus oxycedrus, Pyrus syriaca, Crataegus* spp., *Prunus* and *Amygdalus* spp. (Frey and Kürschner,

105 1989). In the rain-shadow, where rainfall decreases drastically, the northeastern part of the lake drainage is

106 covered by Irano-Turanian steppe vegetation, dominated by *Artemisia fragrans*, steppe forbs and grasses

107 (Zohary, 1973).

3. Material and methods

109 Sedimentary record 'AR' (Ahlat Ridge; 38.667°N, 42.669°E; 357 m water depth) was collected on a

110 bathymetric ridge in the northern part of the Tatvan Basin (Fig. 1B) during the ICDP (International

111 Continental Scientific Drilling Program) project PALEOVAN in summer 2010 (Litt and Anselmetti, 2014;

112 Litt et al., 2012). Here we present data of the uppermost 3.87-41.72 m of the event-corrected composite

113 record (mcblf-nE; depth scale, which excludes volcanic ash layers and mass flow deposits; Stockhecke et

114 al., 2014a), representing the time span from 9.48 to 111.39 ka BP.

3.1 Chronology

116 The chronology of the Lake Van sedimentary sequence is based on an independent proxy records, e.g.,

117 high-resolution XRF measurements (Kwiecien et al., 2014), total organic carbon (TOC; Stockhecke et al.,

118 2014a), and pollen data (Litt et al., 2014), which were used for the construction of the age-depth model as

119 published in Stockhecke et al. (2014a). By adding radiometric dating techniques, the Lake Van

120 chronology was correlated by using 'age control points', derived from visual synchronization with the

121 GICC05-based NGRIP isotope data for this relevant interval (0-116 ka; NGRIP members, 2004;

122 Rasmussen et al., 2006; Svensson et al., 2008; Wolff et al., 2010). Additionally, a correlation with three

123 $^{40}Ar/^{39}Ar$ dated onshore tephra layers was implemented in the age-depth model of the composite profile,

124 i.e. the Nemrut Formation (NF) at 32.70 ± 2.55 ka BP, the Halepkalesi Pumice (HP-10) fallout at 61.60 ±

125 2.55 ka BP as well as the Incekaya-Dibekli Tephra at ~80 ka BP (Stockhecke et al., 2014b; Sumita and

126 Schmincke, 2013). Within the last glacial period, the palaeomagnetic Laschamp excursion at ~41 ka BP

127 (Vigliotti et al., 2014) could be identified in the core sequence. Here we want to stress that, among data

128 sets used for visual correlation, pollen data published in Litt et al. (2014) show the glacial/interglacial

129 changes with the largest signal amplitude. However, the age-depth model of Stockhecke et al. (2014b) is

130 based on tuning with the NGRIP event stratigraphy. The correlation points of the Lake Van sedimentary

131 record have been mainly defined by abiotic proxies (i.e. TOC) caused by a higher time resolution of this

132 data set in comparison to the pollen samples available during that time. Even if we present a high-

133 resolution pollen record in this paper, leads and lags between different biotic and abiotic proxies related to

134 climate events have to be taken into account.

3.2. Palynology

The new high-resolution palynological analyses were performed on 216 sub-samples taken at 10-20 cm intervals. The temporal resolution between each pollen sample, derived from the present age-depth model, is ranging from ~250 years (18.37-21.24 mcblf-nE) to ~500 years (3.87-18.37 and 21.24-41.72 mcblf-nE; Fig. 2).

Pollen samples were processed using standard palynological techniques (Faegri and Iversen, 1993) including chemical treatment with cold 10% HCL, hot 10% KOH, cold 40% HF, acetolysis and final sieving with 10 µm mesh size. In order to calculate the pollen and micro-charcoal (>20µm) concentrations (grains cm^{-3} and particles cm^{-3}, respectively), tablets of *Lycopodium clavatum* (Batch No. 483216, Batch No. 177745) were added to each sample (Stockmarr, 1971).

Pollen identification was carried out to the possible lowest taxonomic level with reference of Beug (2004), Moore et al. (1991), Punt (1976), Reille (1999, 1998, 1995), and the pollen reference collections of the Steinmann-Institute, Department of Palaeobotany. Furthermore, we followed the taxonomic nomenclature after Berglund and Ralska-Jasiewiczowa (1986) and the detailed palynological investigation from the western Iran (van Zeist and Bottema, 1977).

To make these pollen counts statistically representative, a minimum of ~500 identified pollen grains per sub-sample were counted for the calculation of terrestrial pollen percentages (100%), composed of arboreal pollen (AP) and non-arboreal pollen (NAP). Spores of green algae (e.g., *Pediastrum boryanum* spp., *P. simplex*, *P. kawraiskyi*), dinoflagellate cysts, pollen grains of aquatic taxa and damaged pollen grains were excluded from the terrestrial pollen sum and pollen concentration. Percent calculation, cluster analysis to define pollen assemblage zones (PAZ), and construction of the pollen and charcoal diagram (Fig. 2) was carried out by using TILIA program; version 1.7.16 (© 1991-2011 Eric C. Grimm).

3.3 Stable isotope analysis

Lake Van carbonates consist of a mixture of calcite and aragonite precipitated in surface water. We selected 200 sub-samples at the same stratigraphic level which was used for the pollen analysis (20 cm sampling resolution). The freeze-dried and ground sediment samples were analyzed at the University of Kiel using a Finnigan GasBenchII with carbonate option coupled to a DELTAplusXL IRMS. The isotopic composition is given relative to the VPDB standard in the conventional δ-notation and was calibrated against two international reference standards (NBS19 and NBS18). The standard deviation for reference analyses was 0.06 ‰ for the stable isotope signature.

3.4 Profiling measurements

166 Profiling measurements of the complete Lake Van sedimentary record (Ahlat Ridge site) are published
167 and described in detail by Kwiecien et al. (2014) as well as in the high-resolution study of the last
168 interglacial by Pickarski et al. (2015).
169 The sediment cores were scanned with an AVAATECH XRF Core Scanner III at MARUM (Bremen).
170 Intensities of major elements (e.g., Ca, K) on sediment cores were collected every 2 cm down-core over a
171 1 cm² area. The row XRF measurements were processed by the Iterative Least square software (WIN
172 AXIL) package from Canberra Eurisys, providing intensity data in total counts (tc). The Ca/K ratio
173 presented in this paper is unitless.

4. Results

4.1. Palynology

176 The palynological data of the last glacial are presented in Fig. 2. This sequence can be divided into four
177 pollen assemblage superzones (PAS IIa, IIb, IIIa, IIIb) following the criteria described in Tzedakis (1994
178 and references therein), which were applied in Litt et al. (2014) for the low-resolution 600 ka long Lake
179 Van pollen record. The PAS IIa and IIb can be further subdivided into six pollen assemblage zones (PAZ;
180 Fig. 2) based on changes in the AP/NAP ratio and changes in the relative frequency of individual taxa.
181 Main characteristics of each pollen zone and sub-zone as well as criteria for defining the lower boundaries
182 are given in Table 1.
183 The pollen concentration varies between ~2,000 and 40,000 grains cm⁻³ dominated by steppic herbaceous
184 pollen types in particular by *Artemisia* (5-55%), Chenopodiaceae (3-64%), and Poaceae (6-35%). Total
185 arboreal pollen percentages alternate between 0.5 and 67% during the last glacial. The main tree taxa are
186 *Pinus* (0-61%) and deciduous *Quercus* (0-15%), whereby the most indicative temperate taxon is
187 deciduous *Quercus* characterized by relative high percentages during interstadials.
188 Microscopic charcoal concentrations vary between <200 and ~15,000 particles cm⁻³ throughout the last
189 glacial (Fig. 2, 3D). In general, charcoal particles of a size commonly recorded from pollen slides reflect
190 fire on a more regional scale (e.g., Clark et al., 1998; Tinner et al., 1998). Here the Lake Van charcoal
191 record can be divided into two distinct intervals: (I) the glacial/stadial interval, when global temperatures
192 and terrestrial biomass were relative low, the charcoal particles concentration stay low (<1,000 particles
193 cm⁻³), and (II) the early interglacial/interstadial interval, when global temperatures increased and
194 vegetation changed, the charcoal record shows high concentrations (>1,000 particles cm⁻³).

4.2. $\delta^{18}O_{bulk}$ and XRF

196 The oxygen isotopic composition of bulk sediments ($\delta^{18}O_{bulk}$) reflects regional climate changes and local
197 temperature variability. However, the interpretation of $\delta^{18}O_{bulk}$ is complex as it can be influenced by a
198 number of climate variables, such as air and water temperature, seasonality of precipitation, moisture

199 source and precipitation-to-evaporation ratio. According to Litt et al. (2012, 2009) and Lemcke and Sturm
200 (1997), the $\delta^{18}O_{bulk}$ values of carbonates at Lake Van are primarily controlled by evaporation processes.
201 Furthermore, Kwiecien et al. (2014) and Pickarski et al. (2015) mention that changes in seasonal rainfall
202 have a significant effect on lake water isotope values. During the last glacial, the oxygen isotope signature
203 of carbonates was apparently heavier during interstadials and lighter during stadials (Fig. 3B).

204 The presented Ca/K record displays a ratio between authigenic carbonate precipitation and siliciclastic
205 material input from the drainage (Kwiecien et al., 2014). According to Kwiecien et al. (2014), the Ca/K
206 ratio shows higher values ascribed to higher amounts of authigenic carbonate during warmer periods
207 (interstadials/interglacial) and lower values related to increasing detrital input during stadials/glacial (Fig.
208 3C).

209 **5. Discussion**

210 **5.1 Long-term vegetation dynamics at Lake Van**

211 Variations in the orbital configuration of the Earth are responsible for changes in the climate system from
212 one state to another; on millennial timescales, for glacial-interglacial cycles (Berger, 1978; Berger et al.,
213 2007). However, higher frequency oscillations (e.g., Dansgaard-Oeschger events; Dansgaard et al., 1993)
214 are superimposed on the long-term orbitally-driven climate dynamics. These abrupt changes of the climate
215 system are not directly driven by orbital forcing, but can be interpreted as transitions between two states of
216 the inter-hemispheric Atlantic Ocean circulation driven by large-scale thermal and salinity gradients (e.g.,
217 Bond and Lotti, 1995; Cacho et al., 2000, 1999; Chapman and Shackleton, 1999; Hemming, 2004; Hodell
218 et al., 2008; McManus et al., 1999; Rasmussen et al., 2014; Wolff et al., 2010). In particular, changes in
219 the oceanic circulation affected regional and local atmospheric circulation patterns, for example, the
220 strength and position of the westerlies in the Northern Hemisphere, which are responsible for the moisture
221 supply in eastern Anatolia (Akçar and Schlüchter, 2005, Roberts et al., 2008).

222 According to Jessen and Milthers (1928) and Litt et al. (2014), an interstadial stage is an interval of
223 temporary improved climate within a glacial phase, which has been either too short to permit full
224 expansion of thermophilous trees and/or too cold or dry to reach the climate optimum of an interglacial
225 period in the same region. In comparison, stadial stages correspond to cold/dry intervals marked not only
226 by global but also by local ice re-advances (Lowe and Walker, 1984).

227 Below, we will discuss only the most pronounced interstadials (e.g., MIS 5c and 5a) and Dansgaard-
228 Oeschger interstadials (AP >10%; e.g., DO 19, 17-16, 14, 12, 8 and 1), here identified on the basis of the
229 Lake Van pollen record (see also Litt et al., 2014). All other 'warm/wet' phases with lower expansion of
230 temperate trees (AP <10%) are not explicitly mentioned in the following section.

231 **5.1.1 MIS 5e-5a**

The last interglacial at Lake Van (MIS 5e; 131.2-111.5 ka BP; Pickarski et al., 2015) is characterized by an oak steppe-forest during the climate optimum (129.1-124.1 ka BP), while coniferous species (e.g., *Pinus*) dominated the late interglacial period between 124.1 and 111.5 ka BP at the minimum peak in summer insolation (Pickarski et al., 2015; Fig. 3A, E). The expansion of dry-tolerant and/or cold-adapted *Pinus* (probably *Pinus nigra*) going along with a reduction of warm-temperate species (e.g., deciduous oak) demonstrates cooler temperatures and summer-dry conditions during the late interglacial period (Pickarski et al., 2015). In this regard, Litt et al. (2014) argued that positive summer temperature anomalies and negative winter temperature anomalies during the late interglacial lead to a strong continentality, more precisely, to strong temperature variations with still low moisture availability in eastern Anatolia.

MIS 5d is marked by a significant expansion of steppic herbaceous plants at the expense of wooded landscape, which signals a considerable climate deterioration from ~111.5 to 107.8 ka BP (Herning stadial; AP <20%; Fig. 3E). The regional climate at Lake Van was characterized by a strong seasonal moisture deficiency ($\delta^{18}O_{bulk}$ values >2‰, Fig. 3B). The cold/dry climatic conditions with marked seasonality in precipitation during the stadial were responsible for poor soil development and enhanced erosion of regional material as recorded by the Ca/K ratio (Fig. 3C).

An abrupt shift in most proxies (pollen data, $\delta^{18}O_{bulk}$, Ca/K ratio) displays the onset of two pronounced interstadials at 107.8-87.2 ka BP (Brørup interstadial; MIS 5c) and at 84.9-77.5 ka BP (Odderade interstadial; MIS 5a; Fig. 3). The rapid decrease in steppic herbaceous elements (e.g., Chenopodiaceae) and the slow increase of summer-green oaks suggest that climate in eastern Anatolia became progressively warmer and wetter during these interstadials. Similar to the late interglacial stage (124.1-111.5 ka BP), the Brørup interstadial recorded a slight climatic amelioration that continued with the predominance of cold- and/or summer-dry adapted conifers (*Pinus* >60%, Fig. 3E; *Pinus* concentration >20,000 grains cm^{-3}, Fig. 2). Changes in seasonal rainfall inferred from depleted $\delta^{18}O_{bulk}$ values (up to -2‰) to more positive oxygen isotope signatures (>1‰) and generally lower winter temperatures have a decisive negative impact on moisture-requiring thermophilous plants such as deciduous oaks (<10%, Table 1; Fig. 3E). Therefore, the likely occurrence of deciduous *Quercus* in higher altitudes, for instance at southern slopes of the Bitlis Massif, would be caused by increasing orography-related precipitation amounts (Litt et al., 2014). An open oak steppe-forest, which was predominant during the MIS 5e at Lake Van, did not become dominant at any time during the last glacial (Fig. 3E; Pickarski et al., 2015).

The new high-resolution microscopic charcoal data show that fire frequency had an immediate response to climate variability (Fig. 3D). According to previous high-resolution pollen studies by Wick at al. (2003) and Pickarski et al. (2015), rising global temperature and increased moisture availability leads to higher vegetation productivity (e.g., higher vegetation density due to spread of warm-temperate grasslands) that correlates to considerably more fuel for burning during interstadials (>1,000 charcoal particles cm^{-3}; Fig.

267 3D). During stadials, lower microscopic charcoal concentrations (between 300 and 850 particles cm⁻³)

268 characterizes an open dry desert steppe landscape with low vegetation density (e.g., MIS 5b; Daniau et al.,

269 2010; Sadori et al., 2015; Vanniere et al., 2011; Fig. 3D).

270 After a short-term climatic deterioration between ~87.3 to 84.9 ka BP (MIS 5b; Rederstall stadial, AP

271 <10%) characterized by a similar expansion of steppic herbaceous plants as documented for MIS 5d

272 (Herning stadial), the spread of deciduous oaks defined the beginning of the MIS 5a. Environmental

273 conditions of the Odderade interstadial (MIS 5a; ~85-77 ka BP) are difficult to resolve due to the eruption

274 of the Incekaya-Dibekli volcano at ~80 ka BP (Sumita and Schmincke, 2013). The fragmentary

275 documentation of the vegetation signal, primarily due to the respective admixture of pyroclastic material

276 (Stockhecke et al., 2014b), complicates the study of vegetation and climate evolution at Lake Van.

277 Nevertheless, the briefly rising AP level (AP >10%) consisting of deciduous *Quercus*, *Betula* and the

278 sporadic occurrence of *Pistacia* cf. *atlantica*, points to short-term favorable climatic conditions and an

279 increased moisture availability at the beginning of MIS 5a (Fig. 2, 3E). Relatively high fire intensity

280 (charcoal concentration up to 2,000 particles cm⁻³; Fig. 3D) and lower detrital input (Fig. 3C) support an

281 advancing vegetation cover due to warmer climatic conditions. However, *Pinus*, which was dominant

282 during MIS 5c and MIS 5e, is no longer growing in the vicinity of the lake (less than 4%; *Pinus*

283 concentration <200 grains cm⁻³, Fig. 2, 3E). The shift from depleted oxygen isotope signature (-1.90‰) to

284 more positive values (1.81‰, Fig. 3B) confirms the reduction in precipitation and/or increasing

285 evaporation throughout the MIS 5a.

5.2 Abrupt climate changes during MIS 4-2

287 The general dominance of *Artemisia*, Chenopodiaceae, Poaceae and the decrease of arboreal pollen (AP

288 <10%; mainly deciduous *Quercus* and *Pinus*) in the glacial pollen spectra indicate a wide spread of arid

289 desert steppe vegetation in eastern Anatolia between ~75-12 ka BP (Fig. 2, 3). However, the total absence

290 of moisture-requiring thermophilous arboreal species such as *Ulmus* and *Carpinus betulus* or frost-

291 sensitive taxa (e.g., *Pistacia* cf. *atlantica*, evergreen *Quercus*), a low vegetation density, a high terrigenous

292 input (of fluvial and/or eolian origin; Fig. 3C), a consistently positive $\delta^{18}O_{bulk}$ signature (~0.77‰; Fig.

293 3B), and a decreasing microscopic charcoal concentration (from ~1,700 to <400 particles cm⁻³; Fig. 3D)

294 point to a strong aridification and cooling in eastern Anatolia after 70 ka BP. The observation is consistent

295 with low summer insolation (Berger, 1978; Berger et al., 2007), increased global ice volume (Shackleton,

296 1987), and cooler sea surface temperature (SST; Cacho et al., 2000), which, combined with the

297 atmospheric effects of a weakening AMOC (Atlantic Meridional Overturning Circulation; Böhm et al.,

298 2015; Bond et al., 1993) contributed to a widespread aridity across the Mediterranean region (e.g.,

299 Fletcher et al., 2010; Kwiecien et al., 2009; Sánchez Goñi et al., 2002).

300 During MIS 4 to 2, high-frequency vegetation and environmental oscillations in the Lake Van proxies

301 demonstrate a reproducible pattern of centennial to millennial-scale alternation between DO interstadials

302 and DO stadials (Fig. 4; Dansgaard et al., 1993; NGRIP members, 2004; Rasmussen et al., 2014; Sánchez

303 Goñi and Harrison, 2010; Svensson et al., 2006; Wolff et al., 2010). In comparison with the Greenland

304 isotope curve, intervals with lighter δ^{18}O NGRIP values (DO stadials) coincide with lower percentages of

305 AP (Fig. 3E). An increase in deciduous *Quercus* percentages, which is an important criterion for initial

306 warming intervals during Termination 1 (Litt et al., 2014; 2009; Wick et al., 2003) and Termination 2

307 (Pickarski et al., 2015), is characteristic for each DO interstadial (Fig. 3E).

308 In general, the abrupt variability of temperate AP from Lake Van and δ^{18}O NGRIP values are more or less

309 synchronous (Fig. 4). Leads and lags between the proxy records, illustrated in detail in Fig. 5, are difficult

310 to assess due to their heterogeneous resolution. In any case, we cannot expect a perfect matching between

311 biotic and abiotic proxies related to climate events due to their different response time. In addition, the

312 lack of correspondence between the pollen signal and the timing of some DO events could also be

313 explained by uncertainties in the current age-depth model. Still, as expected from various eastern

314 Mediterranean pollen records, the Lake Van pollen record documents that temperate taxa tend to reach

315 their maxima after the onset of a warming phase and, therefore, lag behind the Ca/K increase, which

316 responds immediately to climate changes (Fig. 5).

317 The longest and most pronounced variability of tree populations in the Lake Van pollen record is shown

318 during the MIS 3 (~60-28 ka BP; PAZ IIa3-2) suggesting a rapid alternation of warmer/wetter interstadials

319 and cooler/drier stadials. High-amplitude variations in the Ca/K ratio of Lake Van sediments indicate

320 changes in erosion of regional material, due to unstable environmental condition in the catchment area.

321 Larger interstadials such as DO 19, 17-16, 14, 12, and 8 are indicated by peaks in the Ca/K ratio, which

322 are concurrent with AP maxima and increased regional fire frequency (Fig. 5). As described above, this

323 millennial-scale variability in the proxy record was indirectly modulated by orbital-driven changes and

324 variations in the atmospheric circulation of the Northern Hemisphere (e.g., Cacho et al., 2000, 1999;

325 Chapman and Shackleton, 1999; Hemming, 2004; Hodell et al., 2008; McManus et al., 1999; Rasmussen

326 et al., 2014, Wolff et al., 2010). Consequently, the vegetation and environmental conditions at Lake Van

327 responds to abrupt shifts in temperature and moisture availability related to the position and strength of the

328 westerlies, which brought mild and humid conditions from the North Atlantic into the eastern

329 Mediterranean region (Akçar and Schlüchter, 2005, Allen et al., 1999; Fletcher et al., 2010; Müller et al.,

330 2011; Roberts et al., 2008). The Lake Van δ^{18}O$_{bulk}$ signature supports the suggestion of favorable

331 environment by the receipt of isotopically depleted meltwater supply and/or increased precipitation

332 between ~57 and 54 ka BP (δ^{18}O$_{bulk}$ from -1.21 up to ~1‰; Fig. 3B). Furthermore, we propose that the

333 interval of constantly heavier δ^{18}O$_{bulk}$ values during DO 14 to 12 reflect higher evaporation at Lake Van.

334 The most pronounced DO stadials, i.e. the stadials preceding DO 17, 12, 8, 4, and DO 1 refer to Heinrich

335 events (HE) 6, HE 5, HE 4, HE 3, and HE 1 (Fig., 4A; Bond and Lotti, 1995; Bond et al., 1993; Heinrich,

336 1988). The reduction of oceanic heat transport (weakening or shut down of the AMOC; Böhm et al., 2014;

337 Bond and Lotti, 1995; Bond et al., 1993; Broecker, 1994; Cacho et al., 2000, 1999; Chapman and

338 Shackleton, 1999) led to significantly cooler Mediterranean SST's and climatic conditions in the

339 Mediterranean region (e.g., Allen et al., 1999; Fletcher et al., 2010; Müller et al., 2011; Sánchez Goñi et

340 al., 2002; Tzedakis, 2005; Tzedakis et al., 2004). According to Kwiecien et al. (2009), a decreasing

341 atmosphere-sea surface thermal gradient of the Mediterranean Sea would have caused a reduction in the

342 frequency and strength of storm tracks, which were responsible for an intensifying aridity in the Eastern

343 Mediterranean region. However, since tree populations were already limited at Lake Van during the last

344 glacial (<10% AP), the pollen signal is relatively insensitive to severe climatic deterioration such as

345 Heinrich events. Hence, both types of stadials, Heinrich events and DO stadials, lead to a similar reduction

346 of tree taxa (mainly deciduous *Quercus*), and therefore cannot be clearly distinguished from an average

347 cooling event (Fig. 4B). An exception might be the HE 5 (~49 ka BP; Fig. 4A). A collapse of AP taxa

348 from 10% to less than 2% (Fig. 4B) and a short-term detrital supply (Fig. 3C) show that the climate of HE

349 5 was as cold/dry as the glacial maximum of MIS 4 between 70 and 60 ka BP.

350 Between ~28 and 14 ka BP (PAZ IIa2), very low AP percentages (<10%; Fig. 3E) and a decreasing fire

351 frequency (Fig. 3D) without significant fluctuations underline considerably stable climate conditions but

352 pronounced regional cooling and aridity in comparison to MIS 3. It led to an overall reduction in

353 terrestrial biomass production and thus to a decrease in fuel availability for burning in the catchment area.

354 Furthermore, the presence of *Juniperus*, indicative for an unstable soil cover, enhanced minerogenic input

355 into the lake (low Ca/K; Fig. 3C) and a drop in $\delta^{18}O_{bulk}$ values (up to -1.6‰; Fig. 3B) support the

356 assumption of wide open plains around Lake Van. Insolation changes became the major driver (e.g., low

357 summer insolation, Fig. 3A) and leads to a cooling of global climatic conditions, which results in a

358 maximum ice extent of the Northern Hemisphere during the last glacial maximum (LGM; Cacho et al,

359 2000, 1999; Chapman and Shackleton, 1999; NGRIP members, 2004; Rasmussen et al., 2014; Sánchez

360 Goñi and Harrison, 2010; Wolff et al., 2010).

361 After the LGM (at 21 ± 2 ka; Tzedakis, 2007 and references therein), high summer insolation (Fig. 3A),

362 decreasing global ice volume (Wolff et al., 2010), the resumption of the westerly activity, enhanced

363 precipitation (depleted $\delta^{18}O_{bulk}$ values; Fig. 3B), and locally rising temperatures in eastern Anatolia

364 promoted an expansion of an oak steppe-forest at Lake Van (DO 1 at ~14 ka BP; synonymous with the

365 Bølling-Allerød warm period; Fig. 3E, 4). However, the Late Glacial-Holocene transition (Termination I)

366 was interrupted by the impact of the Younger Dryas (YD) climate reversal between ~12.8 to 11.6 ka BP

367 (Litt et al., 2009; Wick et al., 2003). This dramatic event is characterized by the $\delta^{18}O_{bulk}$ peak (4.46 ‰;

368 Fig. 3B), by the drop of the charcoal concentration (<1,000 particles cm^{-3}; Fig. 3D), and by the rapid

369 increase of arid desert steppe plants (up to 70%; Fig. 2B). Further details about the Late Glacial and early

370 Holocene pollen and microscopic charcoal record of Lake Van are not considered here, as Litt et al.

371 (2009) and Wick et al. (2003) already presented vegetation and inferred environmental conditions for that

372 period.

5.3 Comparison with palynological records from the Mediterranean and Black Sea region

374 A regional comparison between Lake Van and pollen archives from the central (Lago Grande di

375 Monticchio, Italy; Allen et al., 1999) and the eastern Mediterranean regions (Tenaghi Philippon, Greece;

376 Müller et al., 2011), the south eastern Levantine Basin (Core 9509; Langgut et al., 2011), and the Black

377 Sea (Shumilovskikh et al., 2014, 2012) is presented in Fig. 4. Despite differences in elevation, topography

378 and chronology, the palaeoenvironmental investigation indicates a good match based on the similar main

379 trends of the major vegetation elements between the five pollen records. It should be noted that the

380 Monticchio sequence features an independent chronology based on varve counting. Climatic

381 teleconnections between the North Atlantic, Black Sea and different parts of the Mediterranean region are

382 expressed by coeval minima in AP during stadials, suggesting cold and dry conditions and a rather open

383 landscape, in particular in MIS 4 and MIS 2. Between 60 and 45 ka BP, the pollen record from Lake Van

384 reveals a period of increased tree vegetation, which are interpreted as the signature of enhanced

385 precipitation and higher temperature (DO 17-12; Fig. 4B, grey bars). According to Müller et al. (2011),

386 this period was described as the North African Humid Period (NAHP; ca. 55-49 ka BP), where the

387 anatomically modern humans (AMH) migrate from Africa via the Levant to Europe. During that time,

388 climatic conditions in the eastern Mediterranean were more humid and milder as indicated by aa abrupt

389 shift from desert-steppe vegetation to semi-arid grassland at Lake Van (AP ~10%; Fig. 4B) and to open

390 forest vegetation (AP up to 70%, Fig. 4E) in the Tenaghi Philippon area (Müller et al., 2011). The marine

391 pollen record from the south eastern Levantine basin (Fig. 4C) also points to increasing AP percentages

392 during ~56.0 and 44.5 ka BP (Langgut et al., 2011).

393 However, there are some differences between the pollen records. More developed forests exist around the

394 central and eastern Mediterranean Sea and the Black Sea compared to the Near East. Despite the intensive

395 aridification in eastern Anatolia during glacials, the vegetation composition of Lake Van and the

396 Levantine Basin differs from the terrestrial Mediterranean pollen records. Firstly, drought-sensitive taxa

397 such as *Ulmus*, *Carpinus betulus* and *Fagus* were frequently present in Italy, e.g., at Lago Grande di

398 Monticchio, Valle di Castiglione, Stracciacappa and Lagaccione (Allen et al., 1999; Follieri et al., 1998)

399 even during stadials. Secondly, the high-resolution Tenaghi Philippon and Ioannina sequences (Müller et

400 al., 2011; Tzedakis et al., 2002) show that thermophilous trees (deciduous *Quercus*) increased rapidly

401 during each interstadial without migrational lags (Fig. 4G, F). It suggest that these sites were better suited

402 in sustaining refugial temperate tree population due to the effects of orographic precipitation. Thirdly,

403 both the diversity and the low amplitude of variations in temperate tree taxa (e.g., deciduous *Quercus*) of

404 the eastern Mediterranean pollen records (Lake Van and Levantine Basin; Fig. 4C) indicates greater

405 distances and/or slow migration rates from refugia during the glacial interval. Such areas might be found

406 in the south and south-east Black Sea Mountains (Euxinian vegetation) and the Caucasus mountains

407 (Hyrcanian vegetation), which receive increased atmospheric moisture and higher orographic precipitation

408 from the Black Sea (Bottema, 1986; Leroy and Arpe, 2007; Shumilovskikh et al., 2012). Especially the

409 Black Sea region was characterized by mean winter temperatures close to or above 0°C during the last

410 glacial (Shumilovskikh et al., 2014).

411 Moreover, the different vegetation development in the Mediterranean region demonstrates a W-E

412 vegetation gradient from an open temperate forest (including evergreen species) in the central (Allen et al.,

413 1999; Follieri et al., 1998) and eastern Mediterranean (Müller et al., 2011) to a semi-arid grassland in the

414 Near East, where the availability of precipitation is the limiting factor for the establishment of an open oak

415 steppe-forest. This moisture gradient reflects an increasing continental affect and a decreasing influence of

416 changes in the atmospheric circulation of the Northern Hemisphere.

6. Conclusions

418 1. By using a range of paleoenvironmental proxies, we were able to detect subtle climate changes
419   even during generally cold and arid glacial phases. This study illustrates the great potential of
420   Lake Van as an archive of Eastern Mediterranean climate and environment over the entire
421   Quaternary.

422 2. Our new palynological results show the climatic teleconnection between Lake Van and the
423   Atlantic Ocean. It reflects the complex underlying drivers of high frequency regional climate and
424   environmental variability caused by seasonal insolation changes, ice sheet dynamics, and the
425   ocean circulation in the North Atlantic.

426 3. The comparison with central and eastern Mediterranean and Black Sea pollen sequences reveals a
427   W-E gradient of decreasing moisture in the Mediterranean region due to an increasing continental
428   effect and a reduction of the atmospheric impact of the North Atlantic Ocean.

429 4. Dansgaard-Oeschger cycles are clearly recognized in the Lake Van pollen record and by other
430   abiotic proxies. Interstadials are characterized by the spread of temperate vegetation (e.g.,
431   deciduous *Quercus*) suggesting regional moisture availability. Stadials can be recognized by the
432   dominance of steppe elements (e.g., *Artemisia*, Chenopodiaceae) pointing to cold temperature and
433   an increasing aridity.

434 5. Heinrich events cannot clearly be distinguished from an average cooling event (stadials). They
435   show a similar impact on the vegetation and the environment.

436   6. The supply of detrital material seems to respond directly to changes in the vegetation composition,
437   e.g., the terrestrial supply is low (high authigenic carbonate precipitation) when the vegetation
438   cover in the catchment area is dense. In contrast, an open landscape favors a physical erosion
439   including local detrital and dust input.
440   7. Moreover, the fire frequency at Lake Van indicates an immediate link to climate changes. The fire
441   frequency is high when global temperatures and regional moisture levels increase providing a
442   higher terrestrial biomass production.

Data availability

Acknowledgements

References

462 Akçar, N., Schlüchter, C., 2005. Paleoglaciations in Anatolia: A Schematic Review and First Results.
463   Eiszeitalter und Gegenwart 55, 102–121.
464 Allen, J.R., Brandt, U., Brauer, A., Hubberten, H.-W., Huntley, B., Keller, J., Kraml, M., Mackensen, A.,
465   Mingram, J., Negendank, J.F., 1999. Rapid environmental changes in southern Europe during the
466   last glacial period. Nature 400, 740–743. doi:10.1038/23432
467 Allen, J.R.M., Watts, W.A., Huntley, B., 2000. Weichselian palynostratigraphy, palaeovegetation and
468   palaeoenvironment; the record from Lago Grande di Monticchio, southern Italy. EDLP - Med
469   Special 73-74, 91–110. doi:10.1016/S1040-6182(00)00067-7

470 Alvarez-Solas, J., Ramstein, G., 2011. On the triggering mechanism of Heinrich events. Proceedings of
471   the National Academy of Sciences 108, E1359–E1360. doi:10.1073/pnas.1116575108

472 Berger, A., 1978. Long-term variations of daily insolation and Quaternary climate changes. Journal of
473   Atmospheric Sciences 35, 2362–2367. doi:http://dx.doi.org/10.1175/1520-
474   0469(1978)035<2362:LTVODI>2.0.CO;2

475 Berger, A., Loute, M.F., Kaspar, F., Lorenz, S.J., 2007. Insolation During Interglacial, in: Sirocko, F.,
476   Claussen, M., Sánchez Goñi, M.F., Litt, T. (Eds.), The Climate of Past Interglacial. Elsevier,
477   Amsterdam, pp. 13–27.

478 Berglund, B.E., Ralska-Jasiewiczowa, M., 1986. Pollen anaylsis and pollen diagrams, in: Berglund, B.E.,
479   Ralska-Jasiewiczowa, M. (Eds.), Handbook of Holocene Palaeoecology and Palaeohydrology.
480   John Wiley and Sons, pp. 455–484.

481 Beug, H.-J., 2004. Leitfaden der Pollenbestimmung für Mitteleuropa und angrenzende Gebiete. Pfeil,
482   München.

483 Blunier, T., Brook, E.J., 2001. Timing of Millennial-Scale Climate Change in Antarctica and Greenland
484   During the Last Glacial Period. Science 291, 109–112. doi:10.1126/science.291.5501.109

485 Böhm, E., Lippold, J., Gutjahr, M., Frank, M., Blaser, P., Antz, B., Fohlmeister, J., Frank, N., Andersen,
486   M.B., Deininger, M., 2015. Strong and deep Atlantic meridional overturning circulation during
487   the last glacial cycle. Nature 517, 73–76. doi:10.1038/nature14059

488 Bond, G.C., Broecker, W.S., Johnsen, S., McManus, J., Labeyrie, L., Jouzel, J., Bonani, G., 1993.
489   Correlations between climate records from North Atlantic sediments and Greenland ice. Nature
490   365, 143–147. doi:10.1038/365143a0

491 Bond, G.C., Heinrich, H., Broecker, W.S., Labeyrie, L., McManus, J., Andrews, J., Huon, S., Jantschik,
492   R., Clasen, S., Simet, C., Tedesco, K., Klas, M., Bonani, G., Ivy, S., 1992. Evidence for massive
493   discharges of icebergs into the North Atlantic ocean during the last glacial period. Nature 360,
494   245–249.

495 Bond, G.C., Lotti, R., 1995. Iceberg Discharges into the North Atlantic on Millennial Time Scales During
496   the Last Glaciation. Science 267, 1005–1010. doi:10.1126/science.267.5200.1005

497 Bottema, S., 1986. A late quaternary pollen diagram from Lake Urmia (Northwestern Iran). Review of
498   Palaeobotany and Palynology 47, 241–261. doi:10.1016/0034-6667(86)90039-4

499 Broecker, W.S., 1994. Massive iceberg discharges as triggers for global climate change. Nature 372, 421–
500   424. doi:10.1038/372421a0Cacho, I., Grimalt, J.O., Pelejero, C., Canals, M., Sierro, F.J., Flores,
501   J.A., Shackleton, N., 1999. Dansgaard-Oeschger and Heinrich event imprints in Alboran Sea
502   paleotemperatures. Paleoceanography 14, 698–705. doi:10.1029/1999PA900044

503 Cacho, I., Grimalt, J.O., Sierro, F.J., Shackleton, N.J. s, Canals, M., 2000. Evidence for enhanced
504   Mediterranean thermohaline circulation during rapid climatic coolings. Earth and Planetary
505   Science Letters 183, 417–429. doi:10.1016/S0012-821X(00)00296-X

506 Chapman, M.R., Shackleton, N.J., 1999. Global ice-volume fluctuations, North Atlantic ice-rafting events,
507   and deep-ocean circulation changes between 130 and 70 ka. Geology 27, 795–798.
508   doi:10.1130/0091-7613(1999)027<0795:GIVFNA>2.3.CO;2

509 Clark, J.S., Lynch, J., Stocks, B.J., Goldammer, J.G., 1998. Relationships between charcoal particles in air
510   and sediments in west-central Siberia. The Holocene 8, 19–29.
511   doi:10.1191/095968398672501165Daniau, A.-L., Harrison, S.P., Bartlein, P.J., 2010. Fire regimes
512   during the Last Glacial. Quaternary Science Reviews 29, 2918–2930.
513   doi:10.1016/j.quascirev.2009.11.008

514 Dansgaard, W., Johnsen, S.J., Clausen, H.B., Dahl-Jensen, D., Gundestrup, N.S., Hammer, C.U.,
515   Hvidberg, C.S., Steffensen, J.P., Sveinbjörnsdottir, A.E., Jouzel, J., Bond, G., 1993. Evidence for
516   general instability of past climate from a 250-kyr ice-core record. Nature 364, 218–220.

517 Degens, E.T., Kurtman, F., 1978. The Geology of Lake Van. The Mineral Research and Exploration
518   Institute of Turkey, Ankara.

519 Faegri, K., Iversen, J., 1993. Bestimmungsschlüssel für die nordwesteuropäische Pollenflora. Gustav
520   Fischer, Jena.

521 Fletcher, W.J., Sánchez Goñi, M.F., Allen, J.R.M., Cheddadi, R., Combourieu-Nebout, N., Huntley, B.,
522   Lawson, I., Londeix, L., Magri, D., Margari, V., Müller, U.C., Naughton, F., Novenko, E.,

523   Roucoux, K., Tzedakis, P.C., 2010. Millennial-scale variability during the last glacial in
524   vegetation records from Europe. Vegetation Response to Millennial-scale Variability during the
525   Last Glacial 29, 2839–2864. doi:10.1016/j.quascirev.2009.11.015
526 Follieri, M., Giardini, M., Magri, D., Sadori, L., 1998. PALYNOSTRATIGRAPHY OF THE LAST
527   GLACIAL PERIOD IN THE VOLCANIC REGION OF CENTRAL ITALY. Quaternary
528   International 47–48, 3–20. doi:10.1016/S1040-6182(97)00065-7
529 Frey, W., Kürschner, H., 1989. Die Vegetation im Vorderer Orient. Erläuterungen zur Karte A VI 1
530   Vorderer Orient. Vegetation des "Tübinger Atlas des Vorderen Orients"., Reihe A. Tübinger Atlas
531   des Vorderen Orients, Wiesbaden.
532 Heinrich, H., 1988. Origin and consequences of cyclic ice rafting in the Northeast Atlantic Ocean during
533   the past 130,000 years. Quaternary Research 29, 142–152. doi:10.1016/0033-5894(88)90057-9
534 Hemming, S.R., 2004. Heinrich events: Massive late Pleistocene detritus layers of the North Atlantic and
535   their global climate imprint. Reviews of Geophysics 42, RG1005. doi:10.1029/2003RG000128
536 Hodell, D.A., Channell, J.E.T., Curtis, J.H., Romero, O.E., Röhl, U., 2008. Onset of "Hudson Strait"
537   Heinrich events in the eastern North Atlantic at the end of the middle Pleistocene transition (∼640
538   ka)? Paleoceanography 23, PA4218. doi:10.1029/2008PA001591
539 Jessen, A., Milthers, V., 1928. Stratigraphical and paleontological studies of interglacial freshwater
540   deposits in Jutland and Northwest Germany. Danmarks Geologiske Undersøgelse 48, 1–379.
541 Kwiecien, O., Arz, H.W., Lamy, F., Plessen, B., Bahr, A., Haug, G.H., 2009. North Atlantic control on
542   precipitation pattern in the eastern Mediterranean/Black Sea region during the last glacial.
543   Quaternary Research 71, 375–384. doi:10.1016/j.yqres.2008.12.004
544 Kwiecien, O., Stockhecke, M., Pickarski, N., Heumann, G., Litt, T., Sturm, M., Anselmetti, F., Kipfer, R.,
545   Haug, G.H., 2014. Dynamics of the last four glacial terminations recorded in Lake Van, Turkey.
546   Quaternary Science Reviews 104, 42–52. doi:10.1016/j.quascirev.2014.07.001
547 Langgut, D., Almogi-Labin, A., Bar-Matthews, M., Weinstein-Evron, M., 2011. Vegetation and climate
548   changes in the South Eastern Mediterranean during the Last Glacial-Interglacial cycle (86 ka):
549   new marine pollen record. Quaternary Science Reviews 30, 3960–3972.
550   doi:10.1016/j.quascirev.2011.10.016
551 Lemcke, G., Sturm, M., 1997. δ18o and Trace Element Measurements as Proxy for the Reconstruction of
552   Climate Changes at Lake Van (Turkey): Preliminary Results, in: Dalfes, H.N., Kukla, G., Weiss,
553   H. (Eds.), Third Millennium BC Climate Change and Old World Collapse, NATO ASI Series.
554   Springer Berlin Heidelberg, pp. 653–678.
555 Leroy, S.A.G., Arpe, K., 2007. Glacial refugia for summer-green trees in Europe and south-west Asia as
556   proposed by ECHAM3 time-slice atmospheric model simulations. Journal of Biogeography 34,
557   2115–2128. doi:10.1111/j.1365-2699.2007.01754.x
558 Lézine, A.-M., von Grafenstein, U., Andersen, N., Belmecheri, S., Bordon, A., Caron, B., Cazet, J.-P.,
559   Erlenkeuser, H., Fouache, E., Grenier, C., Huntsman-Mapila, P., Hureau-Mazaudier, D., Manelli,
560   D., Mazaud, A., Robert, C., Sulpizio, R., Tiercelin, J.-J., Zanchetta, G., Zeqollari, Z., 2010. Lake
561   Ohrid, Albania, provides an exceptional multi-proxy record of environmental changes during the
562   last glacial-interglacial cycle. Palaeogeography, Palaeoclimatology, Palaeoecology 287, 116–127.
563   doi:10.1016/j.palaeo.2010.01.016
564 Litt, T., Anselmetti, F.S., 2014. Lake Van deep drilling project PALEOVAN. Quaternary Science
565   Reviews 104, 1–7. doi:10.1016/j.quascirev.2014.09.026
566 Litt, T., Anselmetti, F.S., Baumgarten, H., Beer, J., Çagatay, N., Cukur, D., Damci, E., Glombitza, C.,
567   Haug, G., Heumann, G., Kallmeyer, J., Kipfer, R., Krastel, S., Kwiecien, O., Meydan, A.F.,
568   Orcen, S., Pickarski, N., Randlett, M.-E., Schmincke, H.-U., Schubert, C.J., Sturm, M., Sumita,
569   M., Stockhecke, M., Tomonaga, Y., Vigliotti, L., Wonik, T., team, the P. scientific, 2012.
570   500,000 Years of Environmental History in Eastern Anatolia: The PALEOVAN Drilling Project.
571   Scientific Drilling Journal 18–29. doi:10.5194/sd-14-18-2012
572 Litt, T., Krastel, S., Sturm, M., Kipfer, R., Örcen, S., Heumann, G., Franz, S.O., Ülgen, U.B., Niessen, F.,
573   2009. "PALEOVAN", International Continental Scientific Drilling Program (ICDP): site survey
574   results and perspectives. Quaternary Science Reviews 28, 1555–1567.
575   doi:10.1016/j.quascirev.2009.03.002

576 Litt, T., Pickarski, N., Heumann, G., Stockhecke, M., Tzedakis, P.C., 2014. A 600,000 year long
577   continental pollen record from Lake Van, eastern Anatolia (Turkey). Quaternary Science Reviews
578   104, 30–41. doi:10.1016/j.quascirev.2014.03.017
579 Lowe, J.J., Walker, M.J.C., 1984. Reconstructing Quaternary Environments, 2nd ed. Longman,
580   Edinburgh.
581 McManus, J.F., Oppo, D.W., Cullen, J.L., 1999. A 0.5-Million-Year Record of Millennial-Scale Climate
582   Variability in the North Atlantic. Science 283, 971–975. doi:10.1126/science.283.5404.971
583 Moore, P.D., Webb, J.A., Collinson, M.E., 1991. Pollen Analysis. Blackwell Science.
584 Müller, U.C., Pross, J., Tzedakis, P.C., Gamble, C., Kotthoff, U., Schmiedl, G., Wulf, S., Christanis, K.,
585   2011. The role of climate in the spread of modern humans into Europe. Quaternary Science
586   Reviews 30, 273–279. doi:10.1016/j.quascirev.2010.11.016
587 NGRIP members, 2004. High-resolution record of Northern Hemisphere climate extending into the last
588   interglacial period. Nature 431, 147–151. doi:10.1038/nature02805
589 Panagiotopoulos, K., Böhm, A., Leng, M., Wagner, B., Schäbitz, F., 2014. Climate variability over the last
590   92 ka in SW Balkans from analysis of sediments from Lake Prespa. Climate of the Past 10, 643–
591   660. doi:10.5194/cp-10-643-2014
592 Pickarski, N., Kwiecien, O., Djamali, M., Litt, T., 2015. Vegetation and environmental changes during the
593   last interglacial in eastern Anatolia (Turkey): a new high-resolution pollen record from Lake Van.
594   Palaeogeography, Palaeoclimatology, Palaeoecology 435, 145-158.
595   http://dx.doi.org/10.1016/j.palaeo.2015.06.015
596 Punt, W., 1976. The Northwest European Pollen Flora. Elsevier, Amsterdam.
597 Rasmussen, S.O., Andersen, K.K., Svensson, A.M., Steffensen, J.P., Vinther, B.M., Clausen, H.B.,
598   Siggaard-Andersen, M.-L., Johnsen, S.J., Larsen, L.B., Dahl-Jensen, D., Bigler, M., Röthlisberger,
599   R., Fischer, H., Goto-Azuma, K., Hansson, M.E., Ruth, U., 2006. A new Greenland ice core
600   chronology for the last glacial termination. Journal of Geophysical Research: Atmospheres 111,
601   D06102. doi:10.1029/2005JD006079
602 Rasmussen, S.O., Bigler, M., Blockley, S.P., Blunier, T., Buchardt, S.L., Clausen, H.B., Cvijanovic, I.,
603   Dahl-Jensen, D., Johnsen, S.J., Fischer, H., Gkinis, V., Guillevic, M., Hoek, W.Z., Lowe, J.J.,
604   Pedro, J.B., Popp, T., Seierstad, I.K., Steffensen, J.P., Svensson, A.M., Vallelonga, P., Vinther,
605   B.M., Walker, M.J.C., Wheatley, J.J., Winstrup, M., 2014. A stratigraphic framework for abrupt
606   climatic changes during the Last Glacial period based on three synchronized Greenland ice-core
607   records: refining and extending the INTIMATE event stratigraphy. Quaternary Science Reviews
608   106, 14–28. doi:10.1016/j.quascirev.2014.09.007
609 Reille, M., 1995. Pollen et Spores d'Europe et d'Afrique du Nord (Supplement 1). Laboratoire de
610   Botanique Historique et Palynologie, Marseille.
611 Reille, M., 1998. Pollen et Spores d'Europe et d'Afrique du Nord (Supplement 2). Laboratoire de
612   Botanique Historique et Palynologie, Marseille.
613 Reille, M., 1999. Pollen et Spores d'Europe et d'Afrique du Nord. Laboratoire de Botanique Historique et
614   Palynologie, Marseille.
615 Roberts, N., Jones, M.D., Benkaddour, A., Eastwood, W.J., Filippi, M.L., Frogley, M.R., Lamb, H.F.,
616   Leng, M.J., Reed, J.M., Stein, M., Stevens, L., Valero-Garcés, B., Zanchetta, G., 2008. Stable
617   isotope records of Late Quaternary climate and hydrology from Mediterranean lakes: the
618   ISOMED synthesis. Quaternary Science Review 27, 2426 –2441.
619   http://dx.doi.org/10.1016/j.quascirev.2008.09.005
620 Sadori, L., Masi, A., Ricotta, C. (2015). Climate-driven past fires in central Sicily. Plant Biosystems 149,
621   166-173. doi:10.1080/11263504.2014.992996
622 Sánchez Goñi, M.F., Cacho, I., Turon, J.-L., Guiot, J., Sierro, F.J., Peypouquet, J.-P., Grimalt, J.O.,
623   Shackleton, N.J., 2002. Synchroneity between marine and terrestrial responses to millennial scale
624   climatic variability during the last glacial period in the Mediterranean region. Climate Dynamics
625   19, 95–105. doi:DOI 10.1007/s00382-001-0212-x
626 Sánchez Goñi, M.F., Harrison, S.P., 2010. Introduction: Millennial-scale climate variability and
627   vegetation changes during the Last Glacial: Concepts and terminology. Quaternary Science
628   Reviews 29, 2823–2827. doi:10.1016/j.quascirev.2009.11.014

629 Shackleton, N.J., 1987. Oxygen isotopes, ice volume and sea level. Quaternary Science Reviews 6, 183–
630   190. doi:10.1016/0277-3791(87)90003-5
631 Shumilovskikh, L.S., Fleitmann, D., Nowaczyk, N.R., Behling, H., Marret, F., Wegwerth, A., Arz, H.W.,
632   2014. Orbital- and millennial-scale environmental changes between 64 and 20 ka BP recorded in
633   Black Sea sediments. Climate of the Past 10, 939–954. doi:10.5194/cp-10-939-2014
634 Shumilovskikh, L.S., Tarasov, P., Arz, H.W., Fleitmann, D., Marret, F., Nowaczyk, N., Plessen, B.,
635   Schlütz, F., Behling, H., 2012. Vegetation and environmental dynamics in the southern Black Sea
636   region since 18 kyr BP derived from the marine core 22-GC3. Palaeogeography,
637   Palaeoclimatology, Palaeoecology 337-338, 177–193.
638 Stockhecke, M., Kwiecien, O., Vigliotti, L., Litt, T., Pickarski, N., Schmincke, H.-U., Çağatay, N., 2014a.
639   Chronology of the 600 ka old long continental record of Lake Van: climatostratigraphic
640   synchronization and dating. Quarternary Sciences Reviews 104, 8-17.
641   http://dx.doi.org/10.1016/j.quascirev.2014.04.008
642 Stockhecke, M., Sturm, M., Brunner, I., Schmincke, H., Sumita, M., Kipfer, R., Cukur, D., Kwiecien, O.,
643   Anselmetti, F.S., 2014b. Sedimentary evolution and environmental history of Lake Van (Turkey)
644   over the past 600 000 years. Sedimentology 61, 1830-1861. doi: 10.1111/sed.12118
645 Stockmarr, J., 1971. Tablets with spores used in absolute pollen analysis. Pollen et Spores 13, 615–621.
646 Sumita, M., Schmincke, H.-U., 2013. Impact of volcanism on the evolution of Lake Van II: Temporal
647   evolution of explosive volcanism of Nemrut Volcano (eastern Anatolia) during the past ca. 0.4
648   Ma. Journal of Volcanology and Geothermal Research 253, 15–34.
649   doi:10.1016/j.jvolgeores.2012.12.009
650 Svensson, A., Andersen, K.K., Bigler, M., Clausen, H.B., Dahl-Jensen, D., Davies, S.M., Johnsen, S.J.,
651   Muscheler, R., Parrenin, F., Rasmussen, S.O., Röthlisberger, R., Seierstad, I., Steffensen, J.P.,
652   Vinther, B.M., 2008. A 60 000 year Greenland stratigraphic ice core chronology. Climate of the
653   Past 4, 47–57. doi:<hal-00330768>
654 Svensson, A., Andersen, K.K., Bigler, M., Clausen, H.B., Dahl-Jensen, D., Davies, S.M., Johnsen, S.J.,
655   Muscheler, R., Rasmussen, S.O., Röthlisberger, R., Peder Steffensen, J., Vinther, B.M., 2006. The
656   Greenland Ice Core Chronology 2005, 15-42 ka. Part 2: comparison to other records. Critical
657   Quaternary Stratigraphy 25, 3258–3267. doi:10.1016/j.quascirev.2006.08.003
658 Tinner, W., Conedera, M., Ammann, B., Gaggeler, H.W., Gedye, S., Jones, R., Sagesser, B., 1998. Pollen
659   and charcoal in lake sediments compared with historically documented forest fires in southern
660   Switzerland since AD 1920. The Holocene 8, 31–42. doi:10.1191/095968398667205430Türkeş,
661   M., 1996. Meteorological Drought in Turkey: A Historical Perspective, 1930-–93. Drought
662   Network News (1994-2001) 84.
663 Tzedakis, P.C., 2007. Seven ambiguities in the Mediterranean palaeoenvironmental narrative. Quaternary
664   Science Review 26, 2042-2066. doi:10.1016/j.quascirev.2007.03.014
665 Tzedakis, P.C., 2005. Towards an understanding of the response of southern European vegetation to
666   orbital and suborbital climate variability. Quaternary Science Reviews 24, 1585–1599.
667   doi:10.1016/j.quascirev.2004.11.012
668 Tzedakis, P.C., 1994. Hierarchical biostratigraphical classification of long pollen sequences. Journal of
669   Quaternary Science 9, 257–259. doi:10.1002/jqs.3390090306
670 Tzedakis, P.C., Frogley, M.R., Lawson, I.T., Preece, R.C., Cacho, I., de Abreu, L., 2004. Ecological
671   thresholds and patterns of millennial-scale climate variability: The response of vegetation in
672   Greece during the last glacial period. Geological Society of America 32, 109–112.
673   doi:10.1130/G20118.1
674 Tzedakis, P.C., Lawson, I.T., Frogley, M.R., Hewitt, G.M., Preece, R.C., 2002. Buffered Tree Population
675   Changes in a Quaternary Refugium: Evolutionary Implications. Science 297, 2044–2047.
676   doi:10.1126/science.1073083
677 Vanniere, B., Power, M.J., Roberts, N., Tinner, W., Carrión, J., Magny, M., Bartlein, P., Colombaroli, D.,
678   Daniau, A.L., Finsinger, W., Gil-Romera, G., Kaltenrieder, P., Pini, R., Sadori, L., Turner, R.,
679   Valsecchi, V., Vescovi, E., 2011. Circum-Mediterranean fire activity and climate changes during
680   the mid-Holocene environmental transition (8500–2500 cal. BP). Holocene 21, 53-73.
681   doi:10.1177/0959683610384164

682 Vigliotti, L., Channell, J.E.T., Stockhecke, M., 2014. Paleomagnetism of Lake Van sediments: chronology
683   and paleoenvironment since 350 ka. Quaternary Science Reviews 104, 18–29.
684   doi:10.1016/j.quascirev.2014.09.028
685 Wick, L., Lemcke, G., Sturm, M., 2003. Evidence of Lateglacial and Holocene climatic change and
686   human impact in eastern Anatolia: high resolution pollen, charcoal, isotopic and geochemical
687   records from the laminated sediments of Lake Van. The Holocene 13, 665–675.
688   doi:10.1191/0959683603hl653rp
689 Wolff, E.W., Chappellaz, J., Blunier, T., Rasmussen, S.O., Svensson, A., 2010. Millennial-scale
690   variability during the last glacial: The ice core record. Vegetation Response to Millennial-scale
691   Variability during the Last Glacial 29, 2828–2838. doi:10.1016/j.quascirev.2009.10.013
692 van Zeist, W., Bottema, S., 1977. Palynological investigations in western Iran. Palaeohistoria Bussum 19,
693   19–85.
694 Zohary, M., 1973. Geobotanical Foundations of the Middle East. Gustav Fischer Verlag, Swets &
695   Zeitlinger. Stuttgart, Amsterdam.

696
697

698 **Figures**

699 Fig. 1: (A) Location of Lake Van in eastern Anatolia (Turkey) and (B) the bathymetry of Lake Van

700 including the main ICDP drill site Ahlat Ridge (AR, black star). Major cities (black dots) and rivers are

701 represented. The black triangle indicates the positions of the active volcanoes Nemrut and Süphan. The

702 Bitlis Massif in the south reaches up to 3,500 m asl.

703 Fig. 2: Pollen diagram for the analyzed last glacial period from the Ahlat Ridge composite profile plotted

704 against age (ka BP) and depth (event-corrected composite record; mcblf-nE). A 10-fold exaggeration line

705 (gray) is used to show changes in low percentages. PAS – Pollen assemblage superzone; PAZ – Pollen

706 assemblage zone. For the discussion see chapter 5.

707 (A) Shown is an arboreal/non-arboreal ratio (AP/NAP), selected arboreal pollen percentages (AP; gray),

708 selected pollen concentrations (grains cm^{-3}), microscopic charcoal concentration (>20µm; particles cm^{-3})

709 and non-pollen palynomorph concentrations (NPP) such as *Pediastrum*, consisting of *Pediastrum*

710 *boryanum* spp., *P. simplex*, and *P. kawraiskyi* (colonies cm^{-3}), and dinoflagellate concentration (cysts cm^{-3}

711). (B) Shown is an arboreal/non-arboreal ratio (AP/NAP), selected non-arboreal pollen percentages (NAP;

712 gray), and selected pollen concentrations (grains cm^{-3}) of *Artemisia*, Chenopodiacae, and Poaceae (red

713 bars).

714 Fig. 3: Comparative study of the Lake Van palaeoenvironmental sequence encompassing the last glacial-

715 interglacial cycle. (A) Mid-June and Mid-January insolation at 40°N (Berger, 1978; Berger et al., 2007);

716 (B) Lake Van oxygen isotope record ($\delta^{18}O_{bulk}$ in ‰ PDB) of autochthonous precipitated carbonates.

717 Shown is the temperature (T) and the isotopic composition ($\delta^{18}O_w$) of the epilimnion; (C)

718 Calcium/potassium ratio (Ca/K) after Kwiecien et al. (2014); (D) Microscopic charcoal concentration

719 (particles cm^{-3}) from 10-110 ka BP (this study) and from 110-135 ka BP (MIS 5e; Pickarski et al. 2015);

720 (E) Selected Lake Van arboreal pollen percentages (AP, *Pinus*, deciduous *Quercus*) from 10 and 110 ka

721   BP (this study) and from 110-135 ka BP described in Pickarski et al. (2015). MIS - Marine Isotope Stage;

722   PAZ - Pollen assemblage zone.

723   Fig. 4: Regional comparison of vegetation dynamics and climate variability in the central and eastern

724   Mediterranean area and Black Sea region concerning Dansgaard-Oeschger cycles (DO) and Heinrich

725   events (HE). (A) δ^{18}O-profile from NGRIP ice core, Greenland (NGRIP members, 2004), labelled with

726   DO 1 to 19 and HE 1 to HE 6 (Bond et al., 1993); (B) Lake Van arboreal pollen record (AP in %, black

727   line) with 1-fold exaggeration (gray line); (C) Marine arboreal pollen record (Core 9509) obtained from

728   the south-eastern Levantine Basin (south-eastern Mediterranean Sea; Langgut et al., 2011); (D) AP record

729   from the SE Black Sea (core 22-GC3 for the period from 10 to 18 ka BP after Shumilovskikh et al. (2012)

730   and core 25-GC1 for the sequence between 19 and 63 ka BP (Shumilovskikh et al., 2014). (E) Arboreal

731   pollen record from Tenaghi Philippon, Greece (Müller et al., 2011); (F) AP record from Lago Grande di

732   Monticchio, southern Italy (Allen et al., 1999). MIS – Marine Isotope Stage.

733   Fig. 5: The longest Dansgaard-Oeschger events DO 8, DO 12, DO 14, DO 16-17 and DO 19 are plotted in

734   extra graphs, demonstrating a good correlation between the vegetation and environmental dynamics in

735   eastern Anatolia and the δ^{18}O-profile from the Greenland ice core sequences (NGRIP members, 2004);

736   Ca/K ratio after Kwiecien et al. (2014); Microscopic charcoal concentration (particles cm^{-3}, this study);

737   Selected Lake Van arboreal pollen (AP, *Pinus*, deciduous *Quercus* in %, this study). The term 'Steppic

738   taxa' includes only major dry-adapted plants such as Chenopodiaceae and *Artemisia*.

739   **Tables**

740   Table 1: Simplified synoptic description of pollen assemblage superzones (PAS) and zones (PAZ).

741   Fig. 1
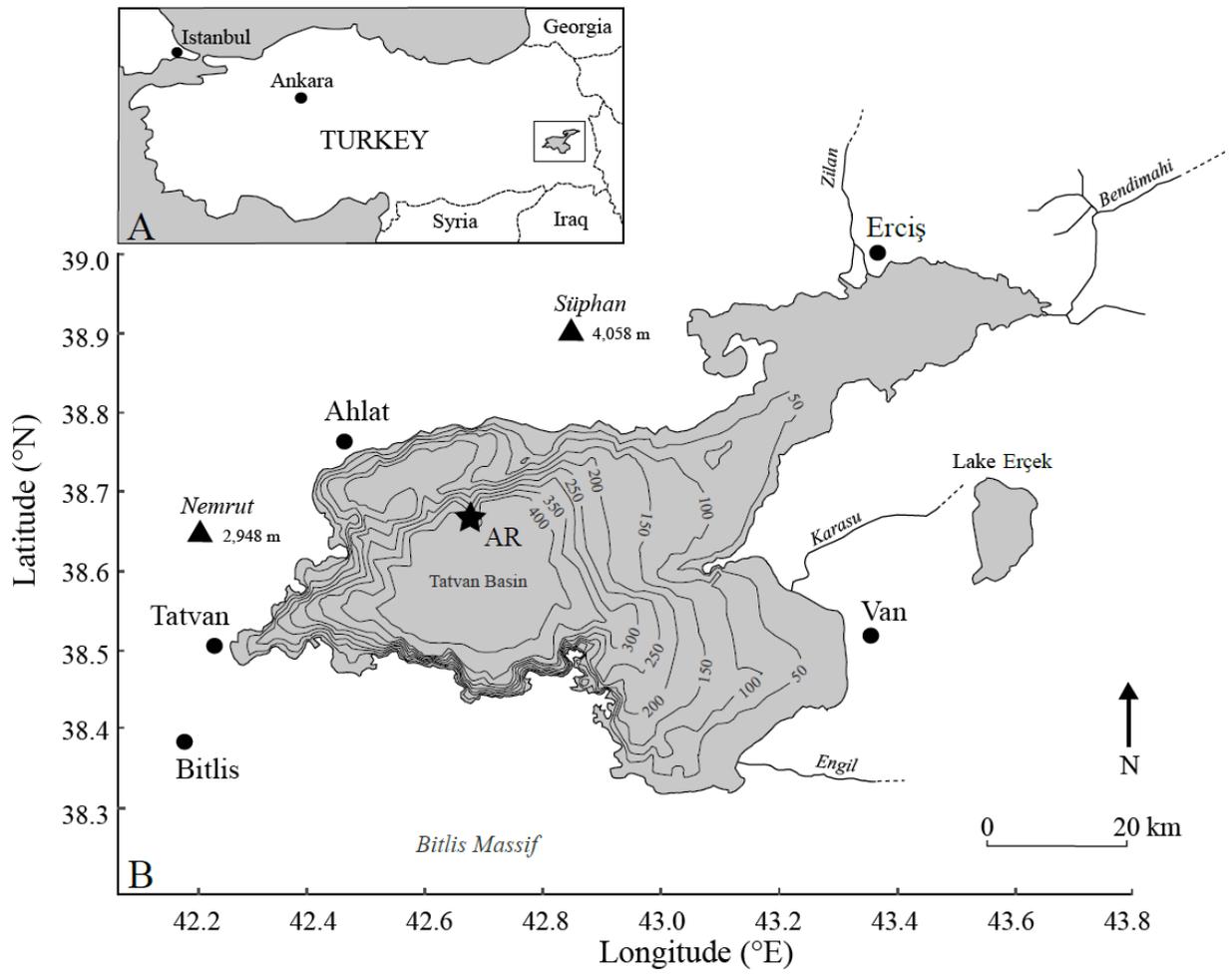
742

743   Fig. 2:
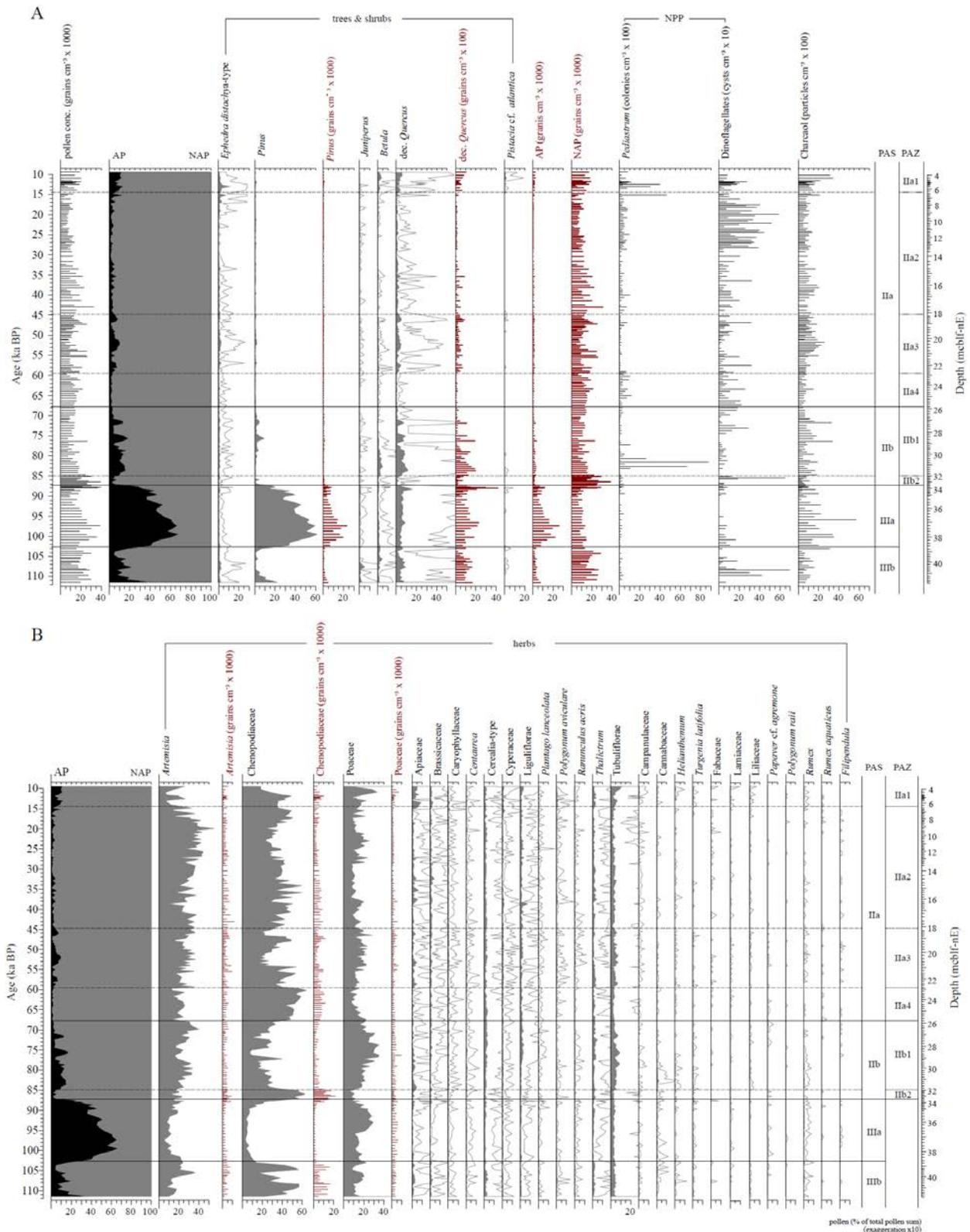
744

745   Fig. 3:
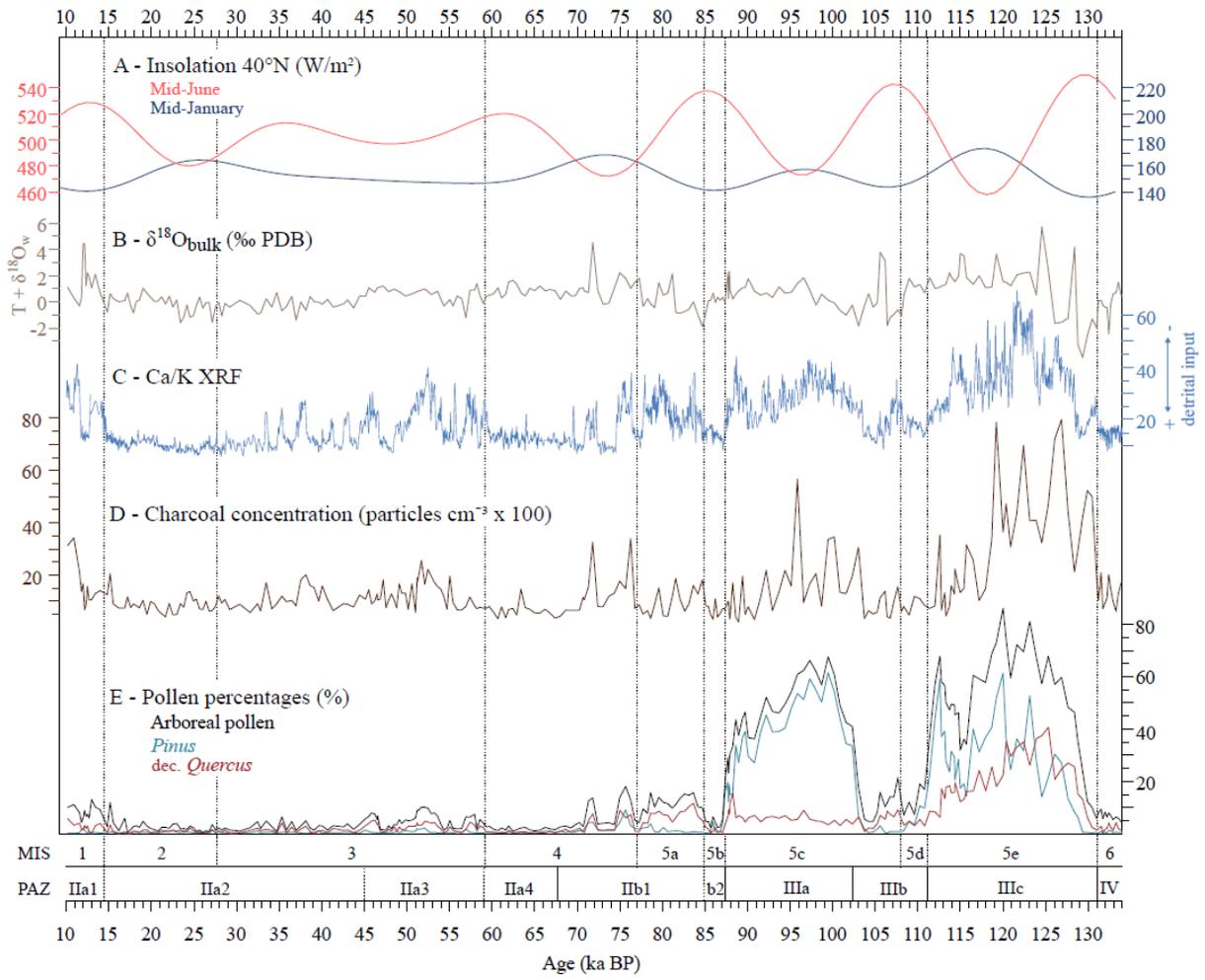
746

747   Fig. 4:
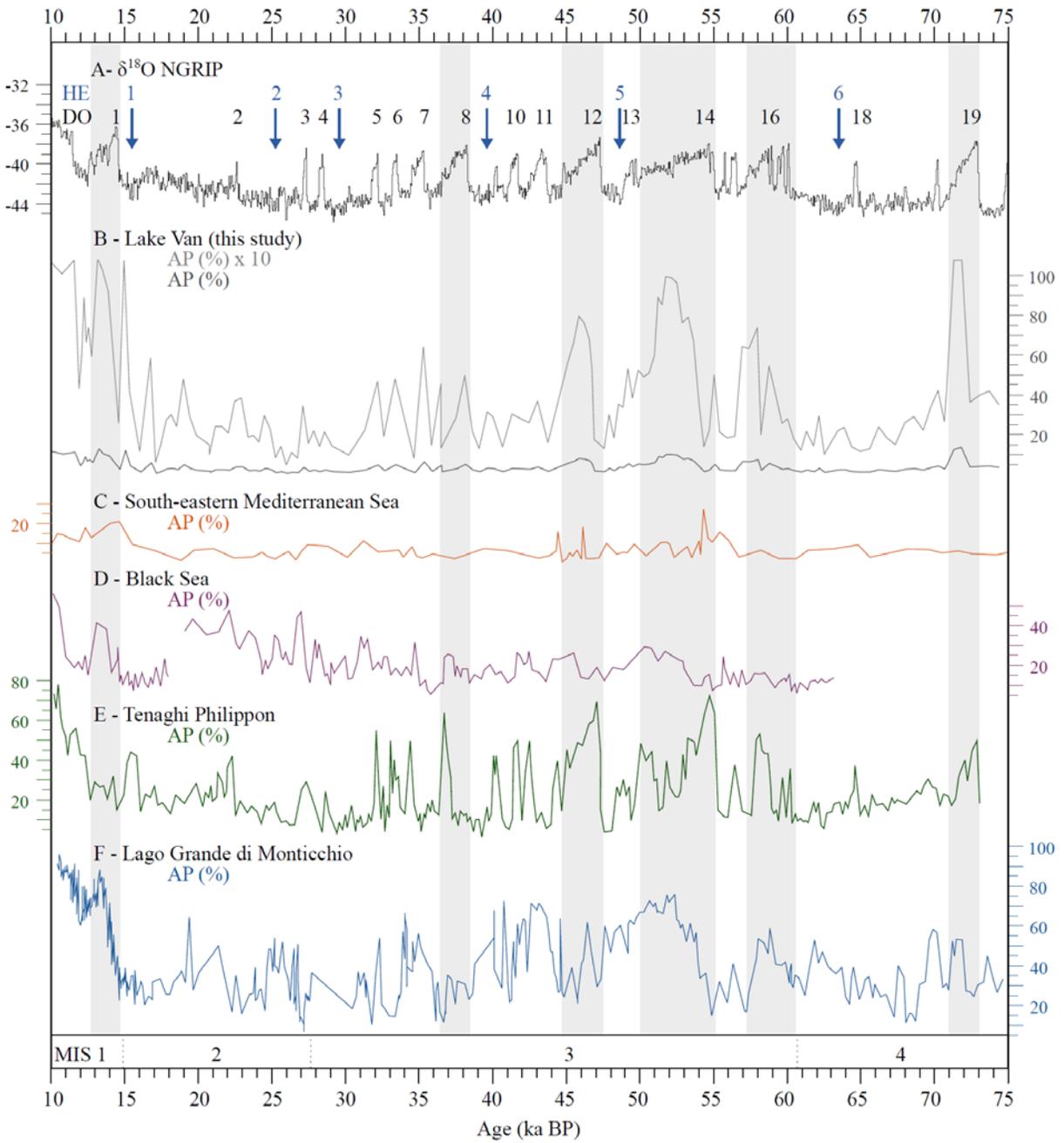
748

749   Fig. 5:

750
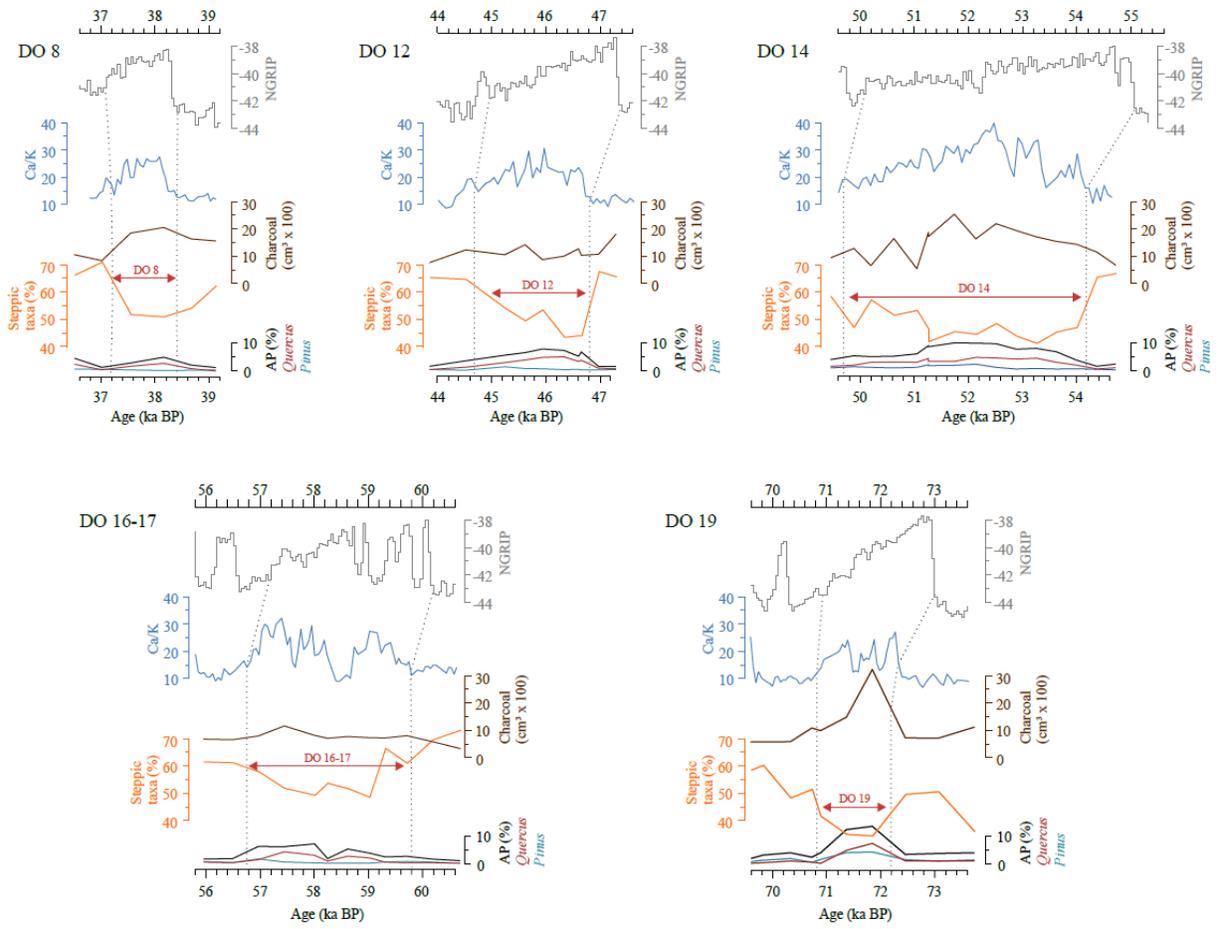
751

752   Table 1:

PAS/ PAZ	Age (ka BP)	Criteria for lower boundary	Pollen assemblages (minimum-maximum in %)
IIa1	09.48 - 14.26	Occurrence of *Pistacia*; *Quercus* >3%	Chenopodiaceae (18-49%) - Poaceae (6-33%) - *Artemisia* (6-33%) - *Ephedra distachya*-type (1-11%) - dec. *Quercus* (0-6%) - *Betula* (0-3%) - *Pistacia* cf. *atlantica* (0-2%) - *Juniperus* (0-1%) - *Pinus* (0-2%)
IIa2	14.26 - 44.80	*Quercus* <2%	Chenopodiaceae (23-60%) - *Artemisia* (10-55%) - Poaceae (7-26%) - *Ephedra distachya*-type (0-7%) - dec. *Quercus* (0-4%) - *Pinus* (0-2%) - *Betula* (0-1%)
IIa3	44.80 - 59.50	*Quercus* >2%; Chenopodiaceae <50%	Chenopodiaceae (15-57%) - *Artemisia* (12-37%) - Poaceae (10-28%) - dec. *Quercus* (0-5%) - *Ephedra distachya*-type (0-3%) - *Betula* (0-2%) - Cyperaceae (0-2%) - *Pinus* (0-2%)
IIa4	59.50 - 67.72	Chenopodiaceae >50%	Chenopodiaceae (29-64%) - *Artemisia* (12-31%) - Poaceae (6-22%) - *Betula* (0-1%) - *Ephedra distachya*-type (0-1%) - *Pinus* (0-1%) - dec. *Quercus* (0-1%)
IIb1	67.72 - 84.91	*Quercus* >5%; Chenopodiaceae <50%	*Artemisia* (16-40%) - Chenopodiaceae (8-57%) - Poaceae (7-35%) - dec. *Quercus* (0-12%) - *Pinus* (0-9%) - *Betula* (0-5%) - *Ephedra distachya*-type (0-2%) - *Juniperus* (0-1%)
IIb2	84.91 - 87.24	*Pinus* <20%; Chenopodiaceae >50%	Chenopodiaceae (44-62%) - *Artemisia* (11-23%) - Poaceae (7-12%) - *Pinus* (0-16%) - dec. *Quercus* (0-4%) - *Betula* (0-1%) - *Ephedra distachya*-type (0-1%)
IIIa	87.24 - 102.67	*Pinus* >20%; Chenopodiaceae <20%	*Pinus* (7-61%) - Poaceae (8-29%) - *Artemisia* (5-25%) - Chenopodiaceae (3-50%) - dec. *Quercus* (3-15%) - *Betula* (0-2%) - *Alnus* (0-1%) - *Ephedra distachya*-type (0-1%) - *Juniperus* (0-1%) - *Pistacia* cf. *atlantica* (0-1%)
IIIb	102.67- 111.70	Chenopodiaceae >20%	Chenopodiaceae (14-57%) - Poaceae (8-22%) - *Artemisia* (7-36%) - dec. *Quercus* (1-9%) - *Pinus* (0-22%) - *Juniperus* (0-5%) - *Betula* (0-4%) - *Ephedra distachya*-type (0-3%) - *Fraxinus* (0-1%) - *Pistacia* cf. *atlantica* (0-1%)

753